Synapses with short-term plasticity are optimal estimators of presynaptic membrane potentials: supplementary note

Jean-Pascal Pfister, Peter Dayan, Máté Lengyel

Supplementary Note

1 The local postsynaptic potential

In the main text we pursue the hypothesis that synapses undergoing STP estimate the somatic membrane potential of the presynaptic cell, with a quantity we called 'the local postsynaptic potential' representing the results of this estimation process. In this section we define the local postsynaptic potential formally. We also explain how experimental data, and in particular those recorded in STP experiments, pertain to it, and how it relates to single neuron computations.

1.1 Biophysical definition

Consider isolating the i^{th} synaptic compartment from the rest of the dendritic tree. If we also ignore any non-synaptic currents, the dynamics of its potential would follow the simple differential equation:

$$C_{\text{m}} \frac{dv^{(i)}}{dt} = \frac{v^{\text{rest}} - v^{(i)}}{R_{\text{m}}} + I^{(i)}_{\text{syn}}(t) \tag{S1}$$

where v^{rest} is the resting membrane potential, C_{m} and R_{m} are the membrane capacitance and resistance, respectively, and $I^{(i)}_{\text{syn}}(t)$ describes the current entering through synaptic channels. We call $v^{(i)}$ the 'local postsynaptic potential'.

1.2 Experimental measurement

Of course, $v^{(i)}$ is an idealization that will not be expressed in either the dendritic or the somatic membrane potential under normal conditions, for at least two reasons. First, the true membrane potential of the local dendritic compartment, $v^{*(i)}$, follows a different equation:

$$C_{\text{m}} \frac{dv^{*(i)}}{dt} = \frac{v^{\text{rest}} - v^{*(i)}}{R_{\text{m}}} + I^{(i)}_{\text{syn}}(t) + I^{(i)}_{\text{other}}(t) \tag{S2}$$

where $I^{(i)}_{\text{other}}(t)$ includes other current contributions that are not the leak current, nor the synaptic current. This includes currents propagated from other parts of the dendritic tree, and active currents generated within the same compartment. Second, $v^{(i)}$ is not expressed in the somatic membrane potential of the post-synaptic neuron, $v^{(\text{soma})}$, because the intervening dendrite filters the synaptic signal, and the soma integrates it with the local postsynaptic potentials created by the many other simultaneously active inputs that the post-synaptic neuron is likely to receive. Therefore, although $v^{(i)}$ is a useful theoretical construct for understanding single neuron computation (as long as Eq. S4 holds, see below), it may not be a quantity that is immediately apparent in membrane potential recordings.

Fortunately for our purposes, STP experiments provide very different conditions from those present in the functional circuit [1], and these make the experimental assessment of $v^{(i)}$ amenable.

In such experiments, which are often *in vitro*[2], normally only a single synapse, or a small subset of synapses is stimulated. This has two effects: the somatic membrane potential depends only on the postsynaptic potential in one dendritic compartment, and the local dendritic membrane potential is kept in the subthreshold regime which minimises the effects of active conductances (i.e. $I_{\text{other}}^{(i)} \approx 0$). Overall, these effects result in the somatic membrane potential reflecting the local postsynaptic potential well except for the consequences of dendritic filtering. Filtering will mostly affect the time constant and absolute amplitude of the somatic signal. We therefore fit only the relative changes in somatic amplitudes (Fig. 3 of the main paper), which should be less affected by this. Nevertheless, a stronger experimental test of the theory would require local dendritic recordings under such minimal stimulation conditions.

1.3 Computational use

A common assumption in models of neural circuit activity is that neurons need to compute some (potentially high-dimensional and complicated) functions of their inputs[3,4]. In terms of (subthreshold) somatic membrane potentials, one can formalise this as

$$v^{(\text{soma})} = \mathcal{F}\Big(u^{(1)}, u^{(2)}, \dots, u^{(M)}\Big) \tag{S3}$$

where $u^{(i)}$ is the somatic membrane potential of presynaptic neuron i (out of M), $v^{(\text{soma})}$ is the somatic membrane potential of the postsynaptic cell, and $\mathcal{F}$ is the non-linear function it computes on its inputs which depends on dendritic processing and other intracellular processes. (Note that Eq. S3 can be rewritten in terms of pre- and postsynaptic firing rates, which are themselves also some non-linear functions of membrane potentials, in the same general form with a suitable choice of $\mathcal{F}$.)

However, since the postsynaptic membrane potential can only directly depend on the spiking output of presynaptic cells, we propose that the cell approximates equation S3 by applying its non-linearity to reliable *estimates* of the presynaptic membrane potentials, $\hat{u}^{(i)}$. These we suggest are represented by the local postsynaptic potentials, $v^{(i)}$ described above:

$$v^{(\text{soma})} = \mathcal{F}\Big(v^{(1)}, v^{(2)}, \dots, v^{(M)}\Big) \simeq \mathcal{F}\Big(\hat{u}^{(1)}, \hat{u}^{(2)}, \dots, \hat{u}^{(M)}\Big) \tag{S4}$$

This is a key reason for introducing $v^{(i)}$ as an idealization. In line with standard reduced neuron models[3,5], we assumed here that the somatic membrane potential can be written to a reasonable approximation in the form given by equation S4 as a function of $v^{(i)}$, rather than $v^{*(i)}$, which means that the effects of $I_{\text{other}}^{(i)}$ are incorporated into $\mathcal{F}$. Crucially, the better the individual $v^{(i)}$ estimate $u^{(i)}$, the better equation S4 implements equation S3. This is illustrated in **Supplementary Figure S1**.

2 Estimation under the switching Ornstein–Uhlenbeck process

2.1 Generative process

For convenience, recall here the description of the generative model under the switching Ornstein–Uhlenbeck (OU) process. In such a process, the resting membrane potential u_t^{rest} is not fixed but randomly switches between two levels, u^+ ans u^-, corresponding to "up" and "down" states (**Supplementary Fig. S2b**)

$$\mathrm{P}\big(u_t^{\text{rest}} | u_{t-\delta t}^{\text{rest}}\big) = \begin{cases} 1-\eta^-\delta t & \text{if } u_t^{\text{rest}} = u^+ \text{ and } u_{t-\delta t}^{\text{rest}} = u^+ \\ \eta^-\delta t & \text{if } u_t^{\text{rest}} = u^- \text{ and } u_{t-\delta t}^{\text{rest}} = u^+ \\ 1-\eta^+\delta t & \text{if } u_t^{\text{rest}} = u^- \text{ and } u_{t-\delta t}^{\text{rest}} = u^- \\ \eta^+\delta t & \text{if } u_t^{\text{rest}} = u^+ \text{ and } u_{t-\delta t}^{\text{rest}} = u^- \end{cases} \tag{S5}$$

where η^- and η^+ are the rates of switching to the "down" and "up" states, respectively. The presynaptic membrane potential evolves as an Ornstein-Uhlenbeck (OU) process around the resting potential u_t^{rest} which is now time-dependent:

$$\mathrm{P}\big(u_t | u_{t-\delta t}, u_t^{\text{rest}}\big) = \mathcal{N}\Big[u_t;\, u_{t-\delta t} + \frac{1}{\tau}\left(u_t^{\text{rest}} - u_{t-\delta t}\right)\delta t,\, \sigma_{\text{W}}^2 \delta t\Big] \tag{S6}$$

Spike generation is described by the same rule as in the non-switching case. See Eqs. 5-7 of the main paper.

2.2 Optimal estimator

The optimal estimator is given by the following filtering equation:

$$\mathrm{P}\big(u_t, u_t^{\mathrm{rest}}|s_{0:t}\big) \propto \mathrm{P}(s_t|u_t) \sum_{u_{t-\delta t}^{\mathrm{rest}}} \int_{-\infty}^{\infty} \mathrm{P}\big(u_t|u_{t-\delta t}, u_t^{\mathrm{rest}}\big)\ \mathrm{P}\big(u_t^{\mathrm{rest}}|u_{t-\delta t}^{\mathrm{rest}}\big)\ \mathrm{P}\big(u_{t-\delta t}, u_{t-\delta t}^{\mathrm{rest}}|s_{0:t-\delta t}\big)\ du_{t-\delta t} \tag{S7}$$

We are primarirly interested in the posterior over the membrane potential. This can be obtained by marginalising Equation S7:

$$\mathrm{P}(u_t|s_{0:t}) = \sum_{u_t^{\mathrm{rest}}} \mathrm{P}\big(u_t, u_t^{\mathrm{rest}}|s_{0:t}\big) = (1-\rho_t)\ p_t^-(u_t) + \rho_t\, p_t^+(u_t) \tag{S8}$$

where

$$\rho_t = \mathrm{P}\big(u_t^{\mathrm{rest}} = u^+|s_{0:t}\big) \tag{S9}$$

is the estimated probability of the resting membrane potential being in its "up" state (or the mixture ratio), and

$$p_t^-(u_t) \quad = \quad \mathrm{P}\big(u_t|u_t^{\mathrm{rest}} = u^-, s_{0:t}\big) \tag{S10}$$

$$p_t^+(u_t) \quad = \quad \mathrm{P}\big(u_t|u_t^{\mathrm{rest}} = u^+, s_{0:t}\big) \tag{S11}$$

express the posterior distribution of u_t assuming that u^{rest} is in its "down" or "up" state, respectively.

The mean of the posterior over the presynaptic membrane potential can be written as:

$$\hat{u}_t = (1-\rho_t)\ \mu_t^- + \rho_t\, \mu_t^+ \tag{S12}$$

where

$$\mu_t^- \quad = \quad \int_{-\infty}^{\infty} u_t\, p_t^-(u_t)\ du_t \tag{S13}$$

$$\mu_t^+ \quad = \quad \int_{-\infty}^{\infty} u_t\, p_t^+(u_t)\ du_t \tag{S14}$$

are the conditional mean estimates of u_t, assuming again that u^{rest} is in its "down" or "up" state, respectively.

The change in the posterior mean, corresponding to postsynaptic potential dynamics (in continuous time) is then

$$\dot{\hat{u}}_t = [1-\rho_{t+\epsilon}]\ \dot{\mu}_t^- + \rho_{t+\epsilon}\, \dot{\mu}_t^+ + \dot{\rho}_t \left[\mu_{t-\epsilon}^+ - \mu_{t-\epsilon}^-\right] \tag{S15}$$

Therefore, there are two factors contributing to changes in the mean posterior (and thus to the size of an EPSP): changes in the conditional means μ^- and μ^+, and changes in the mixture ratio ρ_t. These two factors act additively. However, for closer correspondence with the synaptic resource and utilisation variables (**Online Methods**), Equation S15 can be rearranged as:

$$\dot{\hat{u}}_t = \Delta_t^\mu \left[1 + \frac{\Delta_t^\rho}{\Delta_t^\mu}\right] \tag{S16}$$

where

$$\Delta_t^\mu \quad = \quad [1-\rho_{t+\epsilon}]\ \dot{\mu}_t^- + \rho_{t+\epsilon}\, \dot{\mu}_t^+ \tag{S17}$$

$$\Delta_t^\rho \quad = \quad \dot{\rho}_t \left[\mu_{t-\epsilon}^+ - \mu_{t-\epsilon}^-\right] \tag{S18}$$

correspond to the two factors. The associations of Δ_t^μ and Δ_t^ρ with short-term depression and facilitation respectively are discussed in the two next sections.

2.3 Changes in the conditional means, Δ_t^μ

In order to understand the conditional means, let us first revisit the conditionalised posteriors, $p_t^-(u_t)$ and $p_t^+(u_t)$. In the limit when the dynamics of u^{rest} are sufficiently slow, and u^- and u^+ are not too far apart, these are approximately

$$p_t^-(u_t) \quad \overset{\approx}{\propto} \quad \mathrm{P}(s_t|u_t) \int_{-\infty}^{\infty} \mathrm{P}\big(u_t|u_{t-\delta t}=u', u_t^{\text{rest}}=u^-\big)\; p_{t-\delta t}^-(u')\; du' \tag{S19}$$

$$p_t^+(u_t) \quad \overset{\approx}{\propto} \quad \mathrm{P}(s_t|u_t) \int_{-\infty}^{\infty} \mathrm{P}\big(u_t|u_{t-\delta t}=u', u_t^{\text{rest}}=u^+\big)\; p_{t-\delta t}^+(u')\; du' \tag{S20}$$

If $p_{t-\delta t}^-(u_t)$ and $p_{t-\delta t}^+(u_t)$ are Gaussians, each of Equations S19-S20 describes the posterior updates for a simple OU process with non-linear–Poisson spike generation, as derived in the main paper. This implies that the two conditional means, μ^- and μ^+, evolve as the posterior mean, $\hat{u}$ in Eq. 11 of the main paper: their updates depend on the (here, conditionalised, or relative) posterior variances when observing a spike at time t^*:

$$\dot{\mu}_{t^*}^- \propto \left(\sigma_{t^*-\epsilon}^-\right)^2, \quad \dot{\mu}_{t^*}^+ \propto \left(\sigma_{t^*-\epsilon}^+\right)^2 \tag{S21}$$

where

$$\left(\sigma_t^-\right)^2 = \int_{-\infty}^{\infty} u_t^2\, p_t^-(u_t)\; du_t - \left(\mu_t^-\right)^2 \tag{S22}$$

$$\left(\sigma_t^+\right)^2 = \int_{-\infty}^{\infty} u_t^2\, p_t^+(u_t)\; du_t - \left(\mu_t^+\right)^2 \tag{S23}$$

We know from Eqs. 11 and 12 of the main paper that the proportionality in equation S21 leads to depression. Thus $\Delta_{t^*}^\mu$, the total change in $\hat{u}$ due to changes in the conditional means at the time of an incoming spike t^*, will also show depression because it is a weighted some of two terms that both depress individually:

$$\Delta_{t^*}^\mu \propto \sigma_{t^*}^2 \tag{S24}$$

where, from Eq. S17

$$\sigma_t^2 = [1-\rho_{t+\epsilon}]\; \left(\sigma_{t-\epsilon}^-\right)^2 + \rho_{t+\epsilon}\; \left(\sigma_{t-\epsilon}^+\right)^2 \tag{S25}$$

2.4 Changes in the mixture ratio, Δ_t^ρ

The dynamical equation for the mixture ratio can be derived as (see section 2.5):

$$\dot{\rho}_t \quad \approx \quad \eta^+ - \left[\eta^+ + \eta^- + \gamma_t^+ - \gamma_t^-\right]\; \rho_t - \left[\gamma_t^+ - \gamma_t^-\right]\; \rho_t^2 + \bar{\Delta}_{t-\epsilon}^\rho\, S_t \tag{S26}$$

where

$$\gamma_t^+ \delta t = \mathrm{P}\big(s_t=1|u_t^{\text{rest}}=u^+, s_{0:t-\delta t}\big) \quad \text{and} \quad \gamma_t^- \delta t = \mathrm{P}\big(s_t=1|u_t^{\text{rest}}=u^-, s_{0:t-\delta t}\big) \tag{S27}$$

are the (conditionalised) posterior firing rates and are analogous to γ_t derived in Eq. 10 of the main text.

The most important term from Equation S26 for us now is

$$\bar{\Delta}_{t^*}^\rho = \frac{1}{1+\dfrac{\gamma_{t^*}^-}{\gamma_{t^*}^+}\dfrac{1-\rho_{t^*}}{\rho_{t^*}}} - \rho_{t^*} \tag{S28}$$

expressing the size of the instantaneous update in ρ after observing a spike (Fig. S3) at time t^* (see **Supplementary Figure S3**). This quantity is non-negative, and highly non-linear in ρ: in particular, it has an inverted U-shape which means that in the range of low ρ values (the left arm of the inverted-U), larger ρ values imply larger increments in ρ thus leading to facilitation. The greater the difference in firing rates between the "up" and "down" states is, $\gamma_{t^*}^+/\gamma_{t^*}^-$, the

larger the magnitude but also the smaller the window of facilitation becomes (the peak of the $\bar{\Delta}^{\rho}_{t^*}$ curve shifts up and to the left*). Also note, that for the range of large ρ values, depression, rather than facilitation, is predicted. The overall effect, of course, also depends on the conditional means, because $\Delta^{\rho}_{t^*} = \left[\mu^{+}_{t^*-\epsilon} - \mu^{-}_{t^*-\epsilon}\right] \bar{\Delta}^{\rho}_{t^*}$ (see Eq. S18), and the balance between Δ^{*}_{μ} and Δ^{*}_{ρ} (Eq. S16).

2.5 Deriving $\dot{\rho}$

The mixture ratio $\rho_t = \mathrm{P}(u^{\mathrm{rest}}_t = u^+|s_{0:t})$ at time t can be written as

$$\rho_t = \int_{-\infty}^{\infty} \mathrm{P}\big(u_t, u^{\mathrm{rest}}_t = u^+|s_{0:t}\big)\, du_t \tag{S29}$$

By using the filtering equation of the optimal estimator (equation S7), we write

$$\begin{aligned}
\rho_t \;\propto\; & \sum_{u^{\mathrm{rest}}_{t-\delta t}} \mathrm{P}\big(u^{\mathrm{rest}}_t = u^+|u^{\mathrm{rest}}_{t-\delta t}\big)\, \mathrm{P}\big(u^{\mathrm{rest}}_{t-\delta t}|s_{0:t-\delta t}\big) \cdot \\
& \cdot \int_{-\infty}^{\infty}\int_{-\infty}^{\infty} \mathrm{P}(s_t|u_t)\; \mathrm{P}\big(u_t|u_{t-\delta t}, u^{\mathrm{rest}}_t = u^+\big)\, \mathrm{P}\big(u_{t-\delta t}|u^{\mathrm{rest}}_{t-\delta t}, s_{0:t-\delta t}\big)\, du_{t-\delta t}\, du_t \\
\propto\; & \sum_{u^{\mathrm{rest}}_{t-\delta t}} \mathrm{P}\big(u^{\mathrm{rest}}_t = u^+|u^{\mathrm{rest}}_{t-\delta t}\big)\, \mathrm{P}\big(u^{\mathrm{rest}}_{t-\delta t}|s_{0:t-\delta t}\big) \cdot \qquad \text{(S30)} \\
& \cdot \int_{-\infty}^{\infty} \mathrm{P}\big(s_t|u_{t-\delta t}, u^{\mathrm{rest}}_t = u^+\big)\, \mathrm{P}\big(u_{t-\delta t}|u^{\mathrm{rest}}_{t-\delta t}, s_{0:t-\delta t}\big)\, du_{t-\delta t} \\
\propto\; & \sum_{u^{\mathrm{rest}}_{t-\delta t}} \mathrm{P}\big(u^{\mathrm{rest}}_t = u^+|u^{\mathrm{rest}}_{t-\delta t}\big)\, \mathrm{P}\big(u^{\mathrm{rest}}_{t-\delta t}|s_{0:t-\delta t}\big)\, \mathrm{P}\big(s_t|u^{\mathrm{rest}}_t = u^+, u^{\mathrm{rest}}_{t-\delta t}, s_{0:t-\delta t}\big) \qquad \text{(S31)}
\end{aligned}$$

If we assume that the the probability of having a spike at time t, given the resting membrane potential at time t, u^{rest}_t and the spiking history $s_{0:t-\delta t}$, is independent of the resting membrane potential at time $t - \delta t$, we have:

$$\begin{aligned}
\rho_t \;\overset{\approx}{\propto}\; & \sum_{u^{\mathrm{rest}}_{t-\delta t}} \mathrm{P}\big(u^{\mathrm{rest}}_t = u^+|u^{\mathrm{rest}}_{t-\delta t}\big)\, \mathrm{P}\big(u^{\mathrm{rest}}_{t-\delta t}|s_{0:t-\delta t}\big)\, \mathrm{P}\big(s_t|u^{\mathrm{rest}}_t = u^+, s_{0:t-\delta t}\big) \\
\overset{\approx}{\propto}\; & \mathrm{P}\big(s_t|u^{\mathrm{rest}}_t = u^+, s_{0:t-\delta t}\big)\, \left[(1-\rho_{t-\delta t})\; \eta^+\delta t + \rho_{t-\delta t}\; \left(1-\eta^-\delta t\right)\right] \qquad \text{(S32)}
\end{aligned}$$

Similarly, the estimated probability of being in the "down" state is appoximately proportional (with the same constant of proportionality) to

$$(1-\rho_t) \overset{\approx}{\propto} \mathrm{P}\big(s_t|u^{\mathrm{rest}}_t = u^-, s_{0:t-\delta t}\big)\, \left[(1-\rho_{t-\delta t})\; \left(1-\eta^+\delta t\right) + \rho_{t-\delta t}\, \eta^-\delta t\right] \tag{S33}$$

Let α denote the proportionality factor assumed in equations S32 and S33. By first noting that ρ_t can be trivially rearranged as

$$\rho_t = \frac{1}{1 + \dfrac{\alpha\,(1-\rho_t)}{\alpha\rho_t}} \tag{S34}$$

we can insert equations S32 and S33 to get

$$\rho_t \approx \frac{1}{1 + \dfrac{\mathrm{P}(s_t|u^{\mathrm{rest}}_t = u^-, s_{0:t-\delta t})}{\mathrm{P}(s_t|u^{\mathrm{rest}}_t = u^+, s_{0:t-\delta t})}\, \dfrac{\left[(1-\rho_{t-\delta t})\; (1-\eta^+\delta t) + \rho_{t-\delta t}\, \eta^-\delta t\right]}{\left[(1-\rho_{t-\delta t})\; \eta^+\delta t + \rho_{t-\delta t}\; (1-\eta^-\delta t)\right]}} \tag{S35}$$

*Formally, it can be shown, that $\lim_{\gamma^+_{t^*}/\gamma^-_{t^*}\to\infty} \bar{\Delta}^{\rho}_{t^*} = 1-\rho_{t^*}$ and $\lim_{\gamma^+_{t^*}/\gamma^-_{t^*}\to 1} \bar{\Delta}^{\rho}_{t^*} = \epsilon\,\rho_{t^*}\,[1-\rho_{t^*}]$ where $\epsilon = 1 - \gamma^-_{t^*}/\gamma^+_{t^*} \to 0$. It is interesting to note that in this latter limit the update in ρ happens to be proportional to the uncertainty about the resting membrane potential (i.e. the variance of the associated Bernoulli distribution, $\rho_{t^*}\,[1-\rho_{t^*}]$)

By taking the limit of $\delta t \to 0$ and after some elementary algebra, we can express the temporal derivative of ρ:

$$\begin{aligned}\dot{\rho}_t &= \lim_{\delta t \to 0} \frac{\rho_t - \rho_{t-\delta t}}{\delta t} \\ &\approx \eta^+ - \left[\eta^+ + \eta^- + \gamma_t^+ - \gamma_t^-\right] \rho_t - \left[\gamma_t^+ - \gamma_t^-\right] \rho_t^2 + \bar{\Delta}^\rho_{t-\epsilon} S_t \end{aligned} \tag{S36}$$

where γ_t^+ and γ_t^- denote the conditionalised posterior firing rates of the "up" state and "down" state respectively:

$$\begin{aligned}\gamma_t^+ \delta t &= \mathrm{P}\big(s_t = 1 | u_t^{\mathrm{rest}} = u^+, s_{0:t-\delta t}\big) \\ \gamma_t^- \delta t &= \mathrm{P}\big(s_t = 1 | u_t^{\mathrm{rest}} = u^-, s_{0:t-\delta t}\big)\end{aligned}$$

and $\bar{\Delta}_t^\rho$ denotes the amplitude of the update of ρ after having observed a spike at time t:

$$\bar{\Delta}_t^\rho = \frac{1}{1 + \frac{\gamma_t^-}{\gamma_t^+} \frac{1-\rho_t}{\rho_t}} - \rho_t \tag{S37}$$

Supplementary Figures and Legends

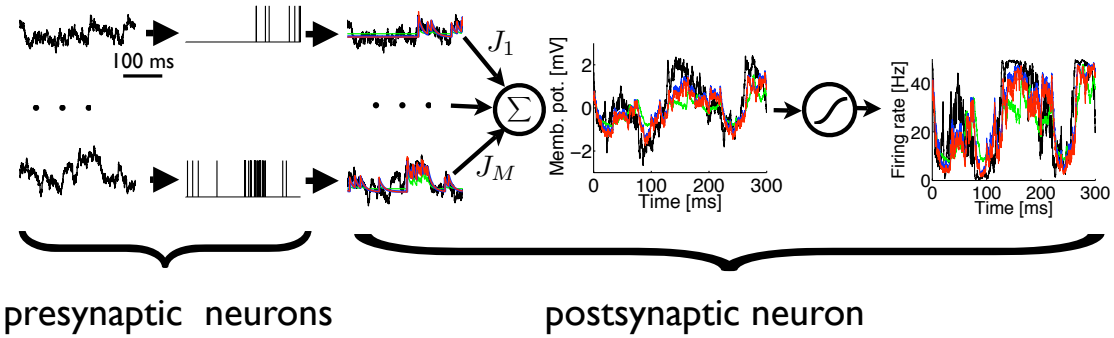

Supplementary Figure S1. Computation with $M = 100$ inputs. Left: membrane potential traces $u^{(i)}$ of the presynaptic neurons. Middle-left: presynaptic spike trains generated from the membrane potential traces. Middle: estimated presynaptic membrane potential $\hat{u}^{(i)}$ with a static synapse (green) a dynamical synapse (blue) and the optimal estimator (red). The black line denotes the presynaptic membrane potential itself. Middle-right: ideally, the somatic membrane potential of the postsynaptic cell computes a (potentially non-linear) function (here, we took $v^{(\text{soma})} = \sum_i J_i u^{(i)}$) of its $M = 100$ inputs (black). Practically, this is approximated as $\sum_i J_i \hat{u}^{(i)}$ with estimates $\hat{u}^{(i)}$ given by static synapses (green), dynamical synapses (blue), or the optimal estimator (red). Right: firing rate of the postsynaptic neuron which is computed as a non-linear (here sigmoidal) function of the somatic potential of the postsynaptic neuron, $f\left(v^{(\text{soma})}\right)$. Parameters for the simulation were: $\beta\sigma = 2$, $\tau = 20$ ms, $g(u^{\text{rest}}) = 10$ Hz, $J_i = 1/\sqrt{M}$, $f(v) = f_0/(1 + \exp(-\alpha v))$, with $f_0 = 50$ Hz and $\alpha = 2$ mV^{-1}.

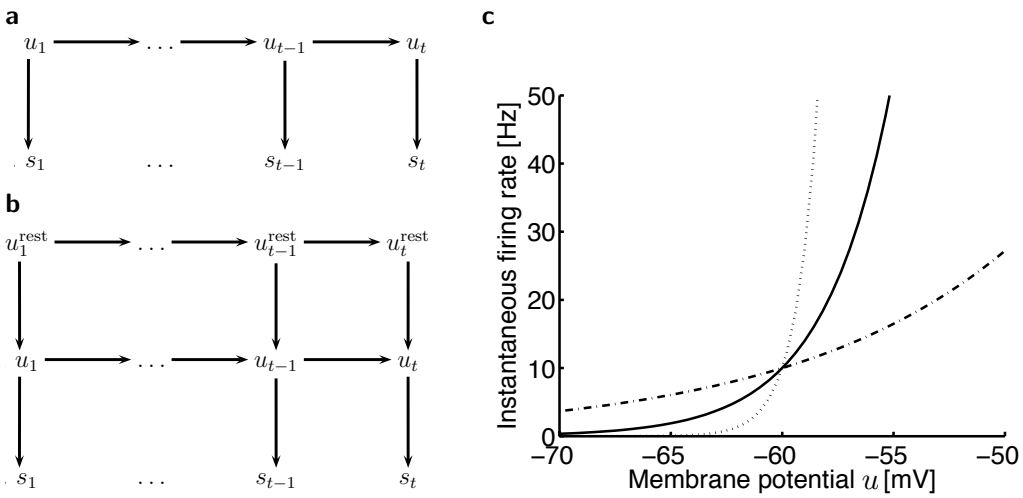

Supplementary Figure S2. Generative model for presynaptic membrane potential fluctuations and spike generation. (**a**) Graphical model for the case with constant resting membrane potential. The membrane potential u_t follows an Ornstein-Uhlenbeck (OU) process around a constant resting potential u^{rest}. A spike is elicited at time t ($s_t = 1$) with probability $g(u_t)\,\delta t$. (**b**) Graphical model for the case with changing resting membrane potential. The resting potential u_t^{rest} (see Eq. S5) can randomly switch between a "down" and an "up" state. (**c**) Instantaneous firing rate $g(u)$ as a function of the membrane potential u for different values of the spiking determinism parameter β ($\beta^{-1} = 3$ mV – solid line, 10 mV – dot-dashed line, 1 mV – dotted line) with g_0 set such that $g(-60\text{ mV}) = 10$ Hz.

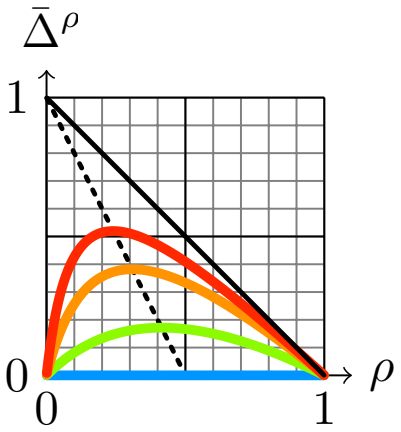

Supplementary Figure S3. $\bar{\Delta}^\rho$, the increment in ρ after observing a spike, as a function of ρ, for different values of $\frac{\gamma_t^+}{\gamma_t^-}$ (1 – blue, 2 – green, 5 – orange, 10 – red, $\to \infty$ - black). Dotted black line shows the location of the peak of the curves as $\frac{\gamma_t^+}{\gamma_t^-}$ is varied $1 \to \infty$.

References

1. Borst, J.G.G. The low synaptic release probability *in vivo*. *Trends Neurosci.* **33**, 259–266 (2010).
2. Dittman, J., Kreitzer, A. & Regehr, W. Interplay between facilitation, depression, and residual calcium at three presynaptic terminals. *J. Neurosci.* **20**, 1374–1385 (2000).
3. Dayan, P. & Abbott, L.F. *Theoretical Neuroscience* (MIT Press, Cambridge, 2001).
4. Zador, A. The basic unit of computation. *Nat. Neurosci.* **3**, 1167 (2000).
5. Aguera y Arcas, B., Fairhall, A.L. & Bialek, W. Computation in a single neuron: Hodgkin and Huxley revisited. *Neural Comput.* **15**, 1715–1749 (2003).